LBL--30889

DE91 016982

Analysis of Polarization Properties of Shallow Metallic Gratings by an Extended Rayleigh-Fano Theory

Masato Koike

Center for X-Ray Optics
Accelerator and Fusion Research Division
Lawrence Berkeley Laboratory
University of California
Berkeley, California 94720

Takeshi Namioka

Research Institute for Scientific Measurements
Tohoku University
Sendai 980
Japan

June 1991

This work was supported by the Director, Office of Energy Research, Office of Basic Energy Sciences, Materials Sciences Division, of the U.S. Department of Energy under Contract No. DE-AC03-76SF00098.

Analysis of polarization properties of shallow metallic gratings by an extended Rayleigh-Fano theory

Masato Koike

Center for X-Ray Optics, Lawrence Berkeley Laboratory
University of California, Berkeley, California 94720

Takeshi Namioka

Research Institute for Scientific Measurements
Tohoku University, Sendai 980, JAPAN

ABSTRACT

Rayleigh-Fano theory has been extended for the purpose of calculating the polarization anomaly of a grating having shallow grooves and finite conductivity. Simple analytic formulas are derived for predicting the position and the appearance of the anomalies. Phenomenological explanations are given to the origin of the anomalies. The validity of our analysis is examined by comparing computed degree of polarization with experimental data obtained in the visible region for Al-, Ag-, and Au-coated blazed gratings.

1. INTRODUCTION

Grating anomalies and their associated problems have been a subject of theoretical interest. The integral and the differential method are capable of solving such problems with the aid of a large computer[1]. However, they have some difficulties in obtaining physical insight into the diffraction process involved. On the other hand, the surface plasmon theory[2,3] gives a physical interpretation on the process, but it is lacking in capability in explaining to a large extent the effect of the groove profile.

Despite the problems in its mathematical formalism, the classical Rayleigh-Fano theory[4-6] is very attractive because it provides a clear physical insight into the diffraction processes involved and permits the use of a personal computer for computation. Therefore, we have extended the Rayleigh-Fano theory and applied it to the analysis of polarization anomalies of shallow metallic gratings.

We outline our extended Rayleigh-Fano theory[7] in Sec. 2. In Sec. 3, we derive simple analytic formulas for predicting the position and the appearance of anomalies and give phenomenological explanations to the origin of the anomalies. We examine the validity of our analysis in Sec. 4 by comparing computed degree of polarization with the data measured in the visible region for Al-, Ag- and Au- coated blazed gratings.

2. EXTENSION OF RAYLEIGH-FANO THEORY

We define a Cartesian coordinate system and the positive direction of angles as shown in Fig. 1. The surface of a plane grating having a period d in the x direction and $z = f(x) = f(x + d)$, divides the whole space into halves; the upper half, U_1, is a vacuum and the lower half, U_2, is composed of the grating material having a complex refractive index $\tilde{n}$. The monochromatic plane wave of wavelength λ travels in a direction perpendicular to the grooves and impinges on the surface at an angle θ. We approximate the fields on both sides of the surface, that is, the incident field $u^{(i)}$, reflected diffraction field $u^{(r)}$, and refracted diffraction field $u^{(t)}$, by superposition of plane waves:

$$
\begin{aligned}
u^{(i)} &= \exp\{ik(x \sin\theta - z \cos\theta)\} , \\
u^{(r)} &= \sum_{m=-\infty}^{\infty} R_m \exp\{ik(x \sin\psi_m + z \cos\psi_m)\} , \\
u^{(t)} &= \sum_{m=-\infty}^{\infty} D_m \exp\{ik\tilde{n}(x \sin\phi_m - z \cos\phi_m)\} ,
\end{aligned}
\tag{1}
$$

where a time dependence of the form $\exp(-i\omega t)$ is implied, ω being the angular frequency of the incident wave. In Eq. (1), $k = 2\pi/\lambda$, ψ_m is the diffraction angle of the reflected mth order diffraction wave, ϕ_m is the diffraction angle of the refracted mth order wave, and R_m and D_m are, respectively, the complex amplitudes of the reflected and refracted mth order diffraction waves.

We express the groove profile in a Fourier series

$$z = f(x) = \sum_{p=-\infty}^{\infty} [a_p \cos(2p\pi x/d) + b_p \sin(2p\pi x/d)] = \sum_{p=1}^{\infty} f_p \exp(-iklpx), \tag{2}$$

where $f_0 = 0$ and $l = \lambda/d$, Using Eqs. (1) and (2), we expand Maxwell's boundary conditions on the grating surface to the second order in $f(x)$. Equating the coefficients of $\exp(-iklmx)$ on both sides of the expanded boundary conditions for a given m, we obtain

$$\begin{aligned} G_{2m}(\cos\psi_m+\beta\cos\phi_m)R_m &= (G_{1m}+H_{1m})\cos\theta - G_{1m}\beta\cos\phi_m - iklmf_m\sin\theta \\ &\quad - \sum_{p\neq m} R_p[(G'_{2mp}+H'_{2mp})\cos\psi_p + G'_{2mp}\beta\cos\phi_m + ikl(m-p)f_{m-p}\sin\psi_p] \\ &\quad - \beta\sum_{p\neq m} D_p[(G'_{3mp}+H'_{3mp})\cos\phi_p - G'_{3mp}\cos\phi_m - ikl(m-p)f_{m-p}\sin\phi_p], \end{aligned} \tag{3}$$

$$\begin{aligned} G_{3m}(\cos\psi_m+\beta\cos\phi_m)D_m &= (G_{1m}+H_{1m})\cos\theta + G_{1m}\cos\psi_m - iklmf_m\sin\theta \\ &\quad - \sum_{p\neq m} R_p[(G'_{2mp}+H'_{2mp})\cos\psi_p - G'_{2mp}\cos\psi_m + ikl(m-p)f_{m-p}\sin\psi_p] \\ &\quad - \sum_{p\neq m} D_p[\beta(G'_{3mp}+H'_{3mp})\cos\phi_p + G'_{3mp}\cos\psi_m - ikl(m-p)f_{m-p}\beta\sin\phi_p], \end{aligned} \tag{4}$$

where $\beta = \bar{n}$ for s component, $\beta = 1/\bar{n}$ for p component. The explicit expressions for G_{im}, G'_{imp}, H'_{imp} ($i = 1, 2, 3$) and H_{1m} in Eqs.(3) and (4) are

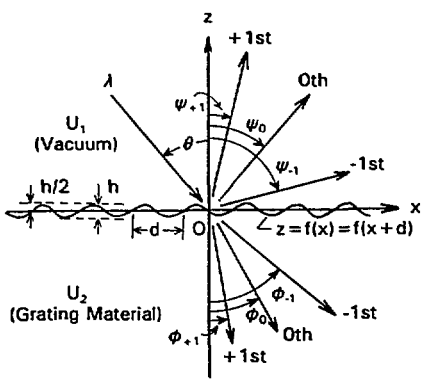

Fig. 1. Diffraction of a plane wave by a plane grating. The angles are taken as positive when measured in the direction indicated by arrows.

$$\begin{aligned} G_{10} &= 1 - \tfrac{1}{2}k^2 g(0)\cos^2\theta , \\ G_{1m} &= -ikf_m\cos\theta - \tfrac{1}{2}k^2 g(m)\cos^2\theta , \quad (m\neq 0) , \\ G_{2m} &= 1 - \tfrac{1}{2}k^2 g(0)\cos^2\psi_m , \\ G'_{2mp} &= ikf_{m-p}\cos\psi_p - \tfrac{1}{2}k^2 g(m-p)\cos^2\psi_p , \\ G_{3m} &= 1 - \tfrac{1}{2}\bar{n}^2 k^2 g(0)\cos^2\phi_m , \\ G'_{3mp} &= -ik\bar{n}f_{m-p}\cos\phi_p - \tfrac{1}{2}k^2\bar{n}^2 g(m-p)\cos^2\phi_p , \\ H_{1m} &= k^2 l h(m)\sin\theta , \\ H'_{2mp} &= k^2 l h(m-p)\sin\psi_p , \\ H'_{3mp} &= k^2 l\bar{n}h(m-p)\sin\phi_p , \end{aligned} \tag{5, 6}$$

where

$$\begin{aligned} g(m) &= \sum_q f_{-q}f_{q+m} , \\ h(m) &= \sum_q q f_{-q}f_{q+m} . \end{aligned} \tag{7}$$

It is noted that both R_m and D_m are expressed as a linear combination of two kinds of terms. One is the functions of quantities associated only with the incident light (λ,β), diffraction order (m), groove profile (d,f_p), grating material $(\bar{n})$, and grating mounting (θ,ψ_m). The other is the terms that represent contributions from diffracted waves (both reflected and refracted) of the other orders. For a mirror, i.e., $f_p=0$, the contributions from all the diffracted waves vanish, and Eqs.(3) and (4) are reduced to Fresnel formulas.

To determine the complex amplitudes R_m and D_m of the diffracted mth order waves from the grating, we employ an iterative method with the initial values given by

$$R_m^{(0)} = \frac{(G_{1m}+H_{1m})\cos\theta - G_{1m}\beta\cos\phi_m - ikl m f_m \sin\theta}{G_{2m}(\cos\psi_m + \beta\cos\phi_m)} \quad , \tag{8}$$

$$D_m^{(0)} = \frac{(G_{1m}+H_{1m})\cos\theta + G_{1m}\cos\psi_m - ikl m f_m \sin\theta}{G_{3m}(\cos\psi_m + \beta\cos\phi_m)} \quad . \tag{9}$$

These initial values are the zero-order solutions obtained by neglecting the contributions from the diffracted p ($\neq m$)th-order waves, i.e., by neglecting the terms containing R_p and D_p ($p \neq m$) in Eqs. (3) and (4). Iterations are carried out by successive approximation: (1) the 1st order solutions $R_m^{(1)}$ and $D_m^{(1)}$ are computed from Eqs.(3)and (4) by substituting the initial values $R_m^{(0)}$'s and $D_m^{(0)}$'s of Eqs.(8) and (9) computed for various m's into R_p's and D_p's, (2) the 2nd order solutions $R_m^{(2)}$ and $D_m^{(2)}$ are computed from Eqs.(3) and (4) by substituting $R_m^{(1)}$'s and $D_m^{(1)}$'s for R_p's and D_p's, and (3) higher-order solutions are obtained successively by repeating steps similar to (2). Iterations are terminated by referring to the degree of convergence of the solution and the energy balance criterion[1]

$$1 = \sum_{m\in U_1} E_m + \sum_{m\in U_2} E'_m \quad . \tag{10}$$

In Eq.(10), E_m and E'_m are the energies of the reflected and the refracted mth-order diffraction waves, respectively, and are expressed by

$$E_m = R_m R_m^* \cos\psi_m/\cos\theta \quad , \quad E'_m = \beta D_m D_m^* \cos\phi_m/\cos\theta \quad , \tag{11}$$

where the asterisk means the complex conjugate.

To examine the validity of our method, we computed P-λ curves, the degree of polarization P vs. wavelength λ,

$$P(m,\lambda) = \frac{[E_m(\lambda)]_s - [E_m(\lambda)]_p}{[E_m(\lambda)]_s + [E_m(\lambda)]_p} \quad , \tag{12}$$

and the energy sums

$$[E(\lambda)]_{s,p} = \sum_{m\in U_1}[E_m(\lambda)]_{s,p} + \sum_{m\in U_2}[E'_m(\lambda)]_{s,p} \quad . \tag{13}$$

3. ANALYSIS OF DIFFRACTION ANOMALIES

A physical picture of the grating anomaly can be drawn by examining the formula for the nth-order solution $R_m^{(n)}$. Applying successive approximations n times, we obtain the complex amplitude $R_m^{(n)}$ of the reflected mth-order diffraction wave:

$$R_m^{(n)} = R_m^{(0)} + \sum_{p\neq m} \frac{F(\lambda,\theta,d,m,p,\beta)}{(\cos\psi_m+\beta\cos\phi_m)(\cos\psi_p+\beta\cos\phi_p)} f_p f_{m-p} + \text{higher orders}, \tag{14}$$

where F is a slowly varying function of λ, θ, d, m, p, and β and is given by

$$F = -k^2\{(\cos^2\theta - \beta\cos\theta\cos\phi_p + lp\sin\theta)[\cos^2\psi_p + \beta\cos\psi_p\cos\phi_m + l(m-p)\sin\psi_p]$$
$$-\beta(\cos^2\theta + \cos\theta\cos\psi_p + lp\sin\theta)[\tilde{n}\cos^2\phi_p - \tilde{n}\cos\phi_p\cos\phi_m + l(m-p)\sin\phi_p]\}. \tag{15}$$

The second term in Eq. (14) represents interactions among the diffracted waves of various orders ($p \neq m$) and the grating structure. These interactions may produce an anomalous effect on the mth-order spectrum under observation if the pth-order wave is either diffracted again(by the grating) or reradiated resonantly (through momentum transfer with the grating) into the mth-order spectrum. This means that in order to have an anomaly, the pth-order wave must be nearly in the state of passing off ($|\sin\psi_p| = 1$) and the factor

$(\cos\psi_p+\beta\cos\phi_p)$ must take a very small value rapidly as ψ_p approaches ±90°.

We observe the mth-order spectrum at a constant angle of incidence while increasing the wavelength λ of the incident light. The factor $(\cos\psi_p+\beta\cos\phi_p)$ is expressed as

$$\cos\psi_p+\beta\cos\phi_p = \{\cos\psi_p+\mathrm{Re}(\beta\cos\phi_p)\} + i\{\mathrm{Im}(\beta\cos\phi_p)\} \quad \text{for} \quad \lambda \le \lambda_R \ (|\sin\psi_p| \le 1) \ , \tag{16}$$

$$\cos\psi_p+\beta\cos\phi_p = \{\mathrm{Re}(\beta\cos\phi_p)\} + i\{|\cos\psi_p|+\mathrm{Im}(\beta\cos\phi_p)\} \text{ for} \quad \lambda > \lambda_R \ (|\sin\psi_p| > 1) \ , \tag{17}$$

where λ_R is the Rayleigh wavelength of the pth-order wave and is defined by

$$p\lambda_R = d(\sin\theta \pm 1) \ . \tag{18}$$

Thus, an anomaly may occur when the real (imaginary) part of Eq. (16) (Eq. (17)) becomes zero at a certain $\lambda \le \lambda_R$ ($\lambda > \lambda_R$).

For p- (s-) polarized incident light, the real (imaginary) parts of Eqs.(16) and (17) are shown to be always positive and are expected to be slowly varying function of λ. The imaginary part of Eq. (16) and the real part of Eq. (17) are also expected to vary slowly with λ. Therefore, no anomaly should occur, within the framework of a shallow grating, at $\lambda \le \lambda_R$ and $\lambda > \lambda_R$, respectively, for the p- and the s-polarized light.

For the p-polarized light, an anomaly associated with the pth-order wave (in a trapped mode within the grating surface) is expected to occur at $\lambda > \lambda_R$ that satisfies

$$|\cos\psi_p| + \mathrm{Im}(\beta\cos\phi_p) = 0 \ , \tag{19}$$

if the following conditions are fulfilled:

$$|\mathrm{Re}(\beta\cos\phi_p)| \ / \ |\mathrm{Im}(\beta\cos\phi_p)| \ll 1 \ , \tag{20}$$

$$\mathrm{Im}(\beta\cos\phi_p) < 0 \text{ and } |d(\cos\psi_p)/d\lambda| > |d[\mathrm{Im}(\beta\cos\phi_p)]/d\lambda| . \tag{21}$$

For the s-polarized light, an anomaly associated with the pth-order wave (in a propagating mode) may occur at $\lambda < \lambda_R$ that satisfies

$$\cos\psi_p + \mathrm{Re}(\beta\cos\phi_p) = 0 \ , \tag{22}$$

if

$$|\mathrm{Im}(\beta\cos\phi_p)| \ / \ |\mathrm{Re}(\beta\cos\phi_p)| \ll 1 \ , \tag{23}$$

$$\mathrm{Re}(\beta\cos\phi_p) < 0 \text{ and } |d(\cos\psi_p)/d\lambda| > |d[\mathrm{Re}(\beta\cos\phi_p)]/d\lambda| . \tag{24}$$

are satisfied. Equations (20) and (23) are the conditions of resonance with a small damping. The second relations in Eqs. (21) and (24) are the conditions necessary for the anomaly to occur in a narrow wavelength range. In the visible range, highly reflective metals have extinction coefficients which are larger than the respective refractive indices. For this reason, Eq. (23) is violated, but Eq. (20) is not. Therefore, shallow metallic gratings do not exhibit anomalies for s-polarized light, but they may show anomalies at $\lambda > \lambda_R$ for p-polarized light if Eqs. (20) and (21) are fulfilled.

4. COMPARISON OF NUMERICAL RESULTS WITH EXPERIMENTAL DATA

4.1. General features of anomalies

To examine the validity of our analysis of the grating anomaly, we compare in this section the numerical results with some experimental data[8] on polarization anomalies of Al-, Ag-, and Au-replica concave gratings having a radius of curvature of 0.5 m, a groove density of 600 grooves/mm, and a blaze angle of 2°35′. Although the experimental data referred to here are on concave gratings, it was shown[8] that the concavity of the grating surface has no influence on the anomalies if the aperture is kept smaller than f/13, thus permitting us to use the data for comparison.

Numerical computations were carried out by using a 80386-SX based personal computer and Basic compiler. In the numerical computations we used the values of optical constants for aluminum[10-12] , silver[13] and gold[14] given in references. The groove profiles of the gratings were approximated by Fourier series of a finite length with $|p| \leq 10$. The degree of polarization was computed for 200 wavelengths in the measured wavelength range of 300 - 700 nm at equal intervals. The energy sum was taken over spectral orders from -10 to 10 for both the s and p components. Under these conditions, it took 6 hours to compute twenty P-λ curves ($m = \pm 1, \pm 2, \cdots, \pm 10$) with five consecutive iterations and the respective energy sums.

Figure 2 shows the measured (open circles) and the computed (solid lines) P-λ curves, the degree of polarization P vs. wavelength λ, of Al-, Ag-, and Au-coated gratings in -1st order at a fixed incident angle of 5°. For reference, the Rayleigh wavelengths are indicated in Fig. 2 (a) by arrows and the associated passing-off orders by numerals. All the P-λ curves shown here are obtained at the first iteration, which is the best compromise as judged by the energy balance criterion. It is clearly seen in Fig. 2 (a) that the general features of the observed anomalies, i.e., the position, shape, and appearance, are well reproduced by the computed curves. Slight discrepancies between the observed and the computed P-λ curves may be attributed to some extent to ambiguity in the values of blaze angle and optical constants used for calculations. In the case of Al-coated grating, rather large deviations seen in the dip positions at short wavelengths are most part due to Al_2O_3 layer formed on the grating surface.

4.2. Position and sharpness of anomalies

To compare the computed results with the observed data more in detail, we take up the P-λ curves of Fig. 2 (a) as a typical example and consider the p-anomalies associated with

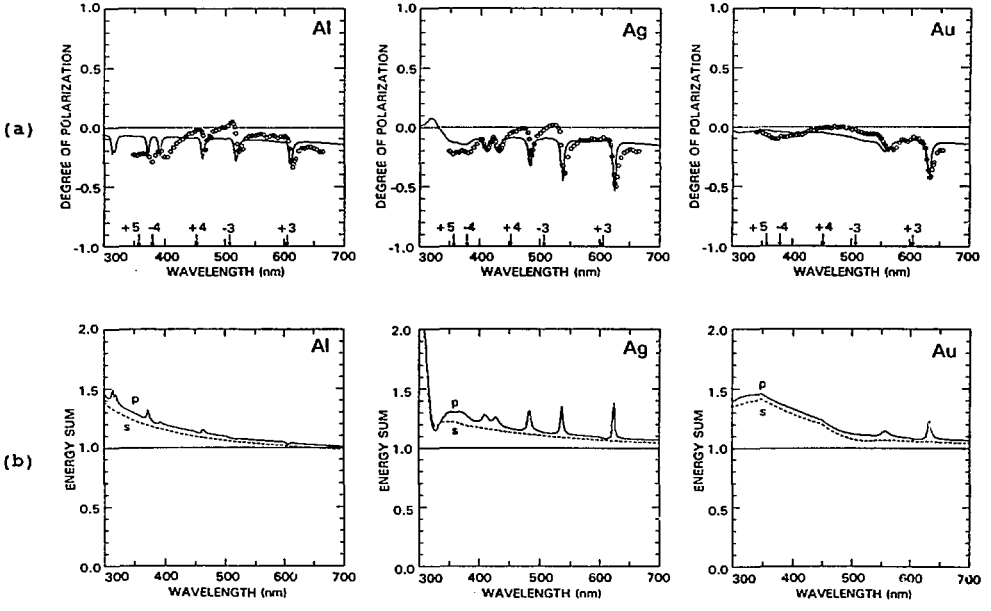

Fig. 2. Computed P-λ curves (a) and the energy sums (b) obtained at the 1st iterations for 600-grooves/mm, 2°35′-blaze, Al-, Ag- and Au-coated ruled concave gratings at a fixed angle of incidence of 5°. The corresponding experimental data-points(o) are shown in (a) for comparison.

passing-off orders of +3 and +4. In this example, we can separate the effect of grating materials from that of groove profiles because the data of Fig. 2 (a) were taken with the gratings replicated in succession from one and the same replica grating using different grating materials.

Figure 3 shows for the Al-, Ag-, and Au-coated gratings the behavior of $-|\cos\psi_p|$ and $\mathrm{Im}(\beta\cos a\phi_p)$ in the vicinity of the Rayleigh wavelength, λ_R = 604.0 nm and 452.9 nm associated, respectively, with the passing-off orders of +3 and +4. As is seen in Fig. 3, the two curves $-|\cos\psi_p|$ and $\mathrm{Im}(\beta\cos\phi_p)$ intersect at a wavelength λ_0. This implies the fulfillment of Eq. (19), suggesting a possibility of observing an anomaly at λ_0 (λ_0's are found to be 611.2, 623.1, and 631.1 nm, in Fig. 3 (a) and 462.8, 482.9, and 503.3 nm in Fig. 3 (b), respectively, for the Al-, Ag-, and Au-coated gratings.

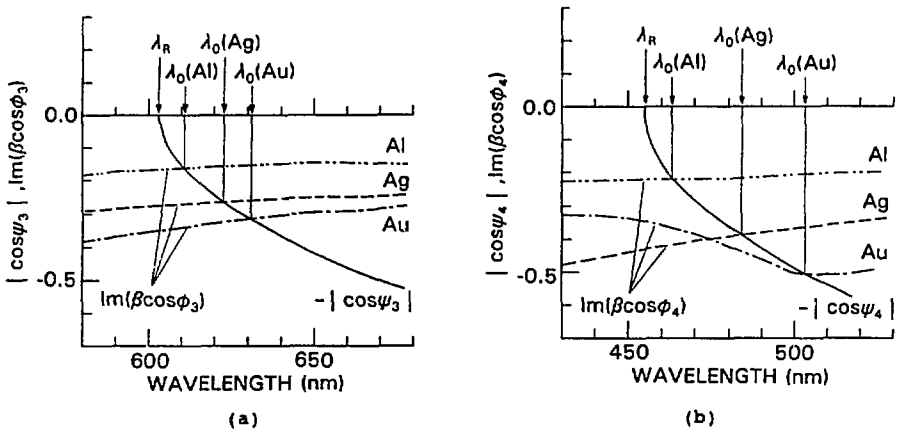

Fig. 3. $-|\cos\psi_p|$ and $\mathrm{Im}(\beta\cos a\phi_p)$ vs. wavelength in the vicinity of anomalies associated with (a) p = +3 and (b) p = +4 for the Al-, Ag-, and Au-coated gratings.

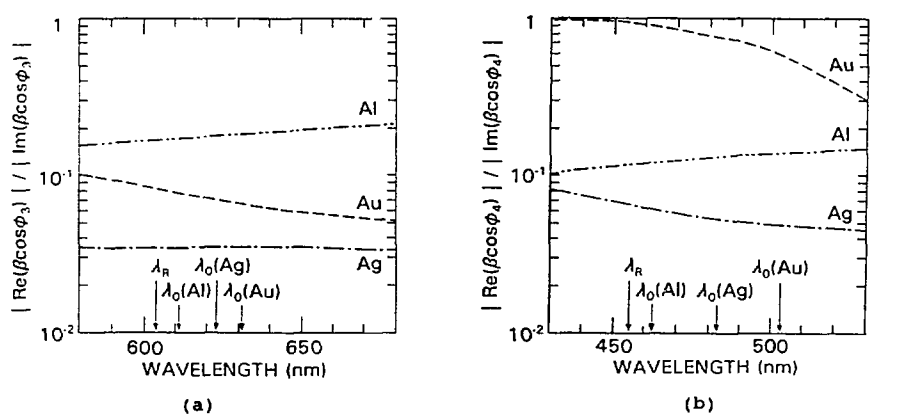

Fig. 4. The magnitude of of $|\mathrm{Re}(\beta\cos\phi_p)|$ / $|\mathrm{Im}(\beta\cos\phi_p)|$ vs. wavelength in the vicinity of anomalies associated with (a) p = +3 and (b) p = +4 for the Al-, Ag- and Au-coated gratings.

The damping effect due to the coating materials (cf. Eq. (20)) should be examined in order to judge whether the anomalies under consideration really appear or not. To do this, we plot $|\mathrm{Re}(\beta\cos\phi_p)|$ / $|\mathrm{Im}(\beta\cos\phi_p)|$ against wavelength as shown in Fig. 4. As to the anomalies associated with p = +3, the damping effect are fairly small for all the gratings (see Fig. 4 (a)), suggesting occurrence of anomalies. The strength of anomalies are estimated, from Fig. 4 (a), to be in order of the Ag-, Au-, and Al-coated gratings. This estimation agrees with the observed result. In the case of p = +4 (Fig. 4 (b)), the Ag- and Al-coated gratings show fairly small damping, whereas the Au-coated grating has strong damping. Therefore, in the case of the Au-coated grating, no anomaly could be excited by the diffracted wave with the passing-off order of +4. This expectation is in agreement with the observed results.

5. CONCLUSION

An attempt has been made to analyze the diffraction anomalies of a grating having shallow grooves and finite conductivity by means of an extended Rayleigh-Fano theory. We derived simple formulas for predicting the wavelength position and the sharpness of anomalies. Considering the theoretical and experimental results obtained, it is concluded that the basic features of the diffraction anomalies can be easily predicted by our method. The theory also provides explanations about the effect of the groove profile on the appearance of anomalies, and this subject will be treated elsewhere.

6. ACKNOWLEDGMENT

This work was partly supported by Material Sciences Division of the U.S. Department of Energy under contract No. DE-AC03-76SF00098.

7. REFERENCES

1. R. Petit, Ed., *Electromagnetic Theory of Gratings*, Topics in Current Physics Vol. 22 (Springer-Verlag, Berlin, 1980).

2. R. H. Ritchie, E. T. Arakawa, J. J. Cowan and R. N. Hamm, "Surface-Plasmon Resonance Effect in Grating Diffraction," Phys. Rev. Letters 21, 1530-1533 (1968).

3. C. E. Wheeler, E. T. Arakawa and R. H. Ritchie, "Photon Excitation of Surface Plasmons in Diffraction Gratings: Effect of groove Depth and Spacing," Phys. Rev. B13, 2372-2376 (1976).

4. Lord Rayleigh, "On the Dynamical Theory of Gratings," Proc. Roy. Soc. (London) A79, 399-416 (1907); see also *Theory of Sound* (Dover Pub., New York, 1945), 2nd ed., Vol.II, Chapt. 13, Sec. 272a,pp. 89-96.

5. U. Fano,"Zur Theorie der Intensitätsanomalien der Beugung," Ann. Phys. 32, 393-443 (1938).

6. U. Fano, "The Theory of Anomalous Diffraction Gratings and of Quasi-Stationary Waves on Metallic Surfaces (Sommerfeld's Waves)," J. Opt. Soc. Am. 31, 213-222 (1941).

7. M. Koike and T. Namioka, "An Extended Rayleigh-Fano Theory and Its Application to Grating Polarization," submitted to Appl. Opt.

8. K. Saito and T. Namioka, "Polarization Anomalies of Concave Gratings," Jpn. J. Appl. Phys. 19, 607-613 (1980).

9.K. Saito, H. Noda and T. Namioka , "Polarization Charactoristics of Concave Gratings Mounted in a Seya-Namioka Monochromator," Opt. Acta 25, 1055-1071 (1978).

10. G. Hass and J. E. Waylonis, "Optical Constants and Reflectance and Transmittance of Evaporated Aluminum in the Visible and Ultraviolet," J. Opt. Soc. Am. 51, 719-722 (1961).

11. L. G. Schulz, "The Optical Constants of Silver, Gold, Copper, and Aluminum. I. The Absorption Coefficient k," J. Opt. Soc. Am. 44, 357-361 (1954).

12.L. G. Suhulz and F. R. Tangherlini, "Optical Constants of Silver, Gold, Copper, and Aluminum. II.The Index of Refraction,"J. Opt. Soc. Am. 44, 362-368 (1954).

13.D. W. Lynch and W. R. Hunter, "Comments on the Optical Constants of Metals and Introduction to the data for Several Metals," in *Handbook of Optical Constants of Solids*, E. D. Palik ed., (Academic Press, Orlando, 1985), pp.275-367.

14.N. Bashara and D. Peterson, "Ellipsometer Study of Anomalous Absorption in Very Thin Dielectric Films on Evaporated Metals," J. Opt. Soc. Am. 36, 1320-1331 (1946).